

Nonlinear variational study of perturbation theory for atoms and ions

F. H. Stillinger and D. K. Stillinger*

Bell Laboratories, Murray Hill, New Jersey 07974

(Received 22 May 1974)

Using the $1/Z$ ($= \lambda$) perturbation format, analytical properties of eigenstates in the complex λ plane have been studied for two- and three-electron atoms, using simple nonlinear variational calculations. The ground states for both systems are included, as well as four excited states for two electrons. The results suggest a general partitioning of bound states into two categories: (i) If the singly charged anion is bound, analytical continuation in λ along the positive real axis causes the energy to penetrate the continuum, and subsequently to terminate at a branch point. (ii) If the singly charged anion is unbound, the energy is tangent to the continuum edge, and analytic continuation in λ to larger positive values creates a non-normalizable wave function.

I. INTRODUCTION

Perturbation theory constitutes one of the most powerful tools available in the study of the quantum mechanics of atoms and molecules. But in spite of widespread application, its basic analytical properties are poorly understood. Our objective in this paper is to illustrate selected important aspects of that version of perturbation theory which treats the full electron-pair interaction as the perturbation. Specifically, we shall be concerned with the ground states of the two- and three-electron atoms, and with four excited states of the former.

In the case of n electrons bound to a nucleus with atomic number Z , the nonrelativistic Hamiltonian may be written in the following reduced manner:

$$H(\lambda) = -\frac{1}{2}(\nabla_1^2 + \cdots + \nabla_n^2) - \frac{1}{r_1} - \cdots - \frac{1}{r_n} + \lambda \sum_{i < j=1}^n \frac{1}{r_{ij}}, \quad \lambda = \frac{1}{Z}. \quad (1.1)$$

Here we have used Z -reduced length and energy units:

$$\begin{aligned} \text{length unit} &= \hbar^2/m_e Z e^2, \\ \text{energy unit} &= m_e Z^2 e^4/\hbar^2. \end{aligned} \quad (1.2)$$

In this formulation the nucleus has been treated as infinitely massive.

The physically realizable cases in (1.1) of course require that λ be the reciprocal of a positive integer. But it is mathematically important to broaden the scope of inquiry to include any arbitrary complex value for the coupling constant λ . The eigenvalues $\epsilon^{(\nu)}(\lambda)$ then may be examined, throughout the complex λ plane, as a set of analytic functions whose singularities become a proper object for attention.

The two-electron ($n=2$) isoelectronic sequence has been studied numerically in great detail. Hyl-

leras¹ was the first to stress the importance of Z^{-1} (i.e., λ) power series for the bound states:

$$\epsilon^{(\nu)}(\lambda) = \sum_{j=0}^{\infty} \epsilon_j^{(\nu)} \lambda^j, \quad (1.3)$$

and he provided accurate values for the first few coefficients $\epsilon_j^{(0)}$ for the ground state. With the advent of modern computing facilities, precise knowledge of these power-series coefficients has advanced dramatically.² In addition, Kato³ has rigorously proved that series (1.3) for the two-electron ground state possesses a nonzero radius of convergence, so that the full set of coefficients $\epsilon_j^{(0)}$ uniquely defines a function $\epsilon^{(0)}(\lambda)$ analytic in the neighborhood of $\lambda=0$.

For any analytic function, the large-order asymptotic behavior of its power-series coefficients is characteristically influenced by the singularities of that function nearest the origin.^{4,5} By using these connections, it has been possible⁶ to infer that $\epsilon^{(0)}(\lambda)$ for the helium isoelectronic sequence ($n=2$) exhibits a branch point, with index approximately $\frac{6}{5}$, at

$$\lambda = \lambda^* \cong 1.1184. \quad (1.4)$$

This is the singularity closest to the origin, and thus its position determines the radius of convergence of the perturbation series. That $\epsilon^{(0)}(\lambda)$ should exceed $-\frac{1}{2}$ (the continuum edge) before λ reaches λ^* while its derivative remains positive has been independently verified,⁷ and this fact provides a contradiction to the orthodox opinion⁸ that the wave function should become infinitely extended as the ionization energy goes to zero.

Although λ power-series coefficients are available for a few helium-sequence excited states,^{2,9} their precise calculation to high-order j is an arduous task. With three or more electrons, the computational requirements are so demanding that no analytical conclusions can currently be drawn

from power series.¹⁰ Development of alternate means to investigate the analytic properties of energy in the complex λ plane therefore seems important.

With this end in mind, we report here the results of some simple nonlinear variational calculations for $n=2$ and 3, which qualitatively exhibit the requisite branch-point behavior for the energy on the positive real axis, in those cases for which this feature has been thought to be present.⁶ It follows from another theorem due to the Kato¹¹ that linear variational approximations with a finite basis are incapable of producing this behavior.

Section II is devoted exclusively to discussion of the two-electron ground state. This is followed in Sec. III by presentation of corresponding results for four excited states of the same system, each the lowest state of a given symmetry. The three-electron ground-state variational results appear in Sec. IV. A wide range of issues raised by the present general inquiry into analytic perturbation theory is discussed in the final Sec. V.

II. TWO-ELECTRON GROUND STATE

Since $H(\lambda)$, Eq. (1.1), is spin independent, it is generally possible to restrict attention to the spatial part of the wave function, provided that this part is suitably constrained. The two-electron ground state is conventionally designated $(1s)^2^1S$, and its spatial part must be symmetric with respect to interchange of electron positions.

For reasons of analytical convenience, we have chosen to work with the Hylleraas-Eckart-Chandrasekhar¹²⁻¹⁴ wave function:

$$\psi(\vec{r}_1, \vec{r}_2) = e^{-\alpha r_1 - \beta r_2} + e^{-\beta r_1 - \alpha r_2}. \quad (2.1)$$

The orbital exponents α and β were regarded as a pair of nonlinear variational parameters with re-

spect to which the variational energy should be minimized for every value of the perturbational coupling constant λ .

When λ vanishes, the exact eigenfunction of $\bar{H}(0)$ is obtained when $\alpha = \beta = 1$, for which $\epsilon^{(0)}(0) = -1$. For nonzero λ , the variational wave function (2.1) only provides an approximation to the exact spatial eigenfunction of $H(\lambda)$, but its flexibility in being able to permit $\alpha \neq \beta$ incorporates radial correlation between the two electrons. Its principal shortcoming is failure to describe angular correlation. However, more extensive calculations which do include angular correlation¹⁵ clearly show that the effects of primary concern in this paper are not drastically altered by that omission.

The variational energy expression for wave function (2.1) is a rational function of α , β , and λ :

$$\begin{aligned} \epsilon(\alpha, \beta, \lambda) &= \int d\vec{r}_1 d\vec{r}_2 \psi H(\lambda) \psi / \int d\vec{r}_1 d\vec{r}_2 \psi^2, \\ &= [F_1(\eta)\alpha^2 + F_2(\eta, \lambda)\alpha] / F_3(\eta). \end{aligned} \quad (2.2)$$

Here we have set

$$\eta = \beta/\alpha, \quad (2.3)$$

and

$$\begin{aligned} F_1(\eta) &= (1+\eta)^6(1+\eta^2) + 128\eta^4, \\ F_2(\eta, \lambda) &= (1+\eta)[2\lambda\eta(1+\eta)^2(1+3\eta+\eta^2) \\ &\quad + 40\lambda\eta^3 - 2(1+\eta)^6 - 128\eta^3], \\ F_3(\eta) &= 2(1+\eta)^6 + 128\eta^3. \end{aligned} \quad (2.4)$$

The way in which $\epsilon(\alpha, \beta, \lambda)$ has been written in Eq. (2.2) arbitrarily singles out α as a common scale factor in ψ . That α should appear only quadratically for fixed η is a general feature, and we know that minimization of ϵ with respect to α , holding η constant, will automatically cause the virial theorem to be satisfied.¹⁶ The value of α which achieves the minimum is the following:

$$\alpha = \frac{(1+\eta)\{\lambda[\eta(1+\eta)^2(1+3\eta+\eta^2) + 20\eta^3] - (1+\eta)^6 - 64\eta^3\}}{(1+\eta)^6(1+\eta^2) + 128\eta^4}. \quad (2.5)$$

This expression may next be used to eliminate α from Eq. (2.2), resulting in an energy function $\epsilon(\eta, \lambda)$ that subsequently needs only to be minimized with respect to η :

$$\epsilon(\eta, \lambda) = - \frac{(1+\eta)^2\{\lambda[\eta(1+\eta)^2(1+3\eta+\eta^2) + 20\eta^3] - (1+\eta)^6 - 64\eta^3\}^2}{2[(1+\eta)^6(1+\eta^2) + 128\eta^4][(1+\eta)^6 + 64\eta^3]}. \quad (2.6)$$

Our numerical analysis has been devoted to the study of Eq. (2.6), for selected λ values, in a direct search for minima and maxima with respect to η variation. Owing to the fact that the starting wave function (2.1) is symmetric in α and β , $\epsilon(\eta, \lambda)$

has turned out to be invariant under replacement of η by η^{-1} . It suffices then to restrict attention to $|\eta| \leq 1$, since any extremum η in this domain automatically has a partner η^{-1} which is also an extremum of the same kind.

Figure 1 shows the extremal real η values as functions of real, positive λ . The branch beginning at $\eta=1$ for $\lambda=0$, and declining monotonically as λ increases, corresponds to the "physical" minimum in $\epsilon(\eta, \lambda)$. It is this branch whose energy values at $\lambda=1, \frac{1}{2}, \frac{1}{3}, \frac{1}{4}, \dots$ represent variational approximations to the ground-state energies of $H^-, He, Li^+, Be^{++}, \dots$. It ends with a vertical tangent at point B in Fig. 1, for which

$$\lambda(B) = 1.078\ 0113, \quad (2.7)$$

and this is the point at which confluence with an energy maximum branch occurs.

A total of four extremum branches are shown in Fig. 1. As η declines from 1, they may be continuously traced out, with alternating minimum and maximum branches, in the order $ABCD$. In addition to point B , vertical-tangent confluences occur at

$$\lambda(C) = 0.993\ 296, \quad \lambda(D) = 1.4283. \quad (2.8)$$

It is interesting to note that the minimum branch CD passes through the point $\lambda=1, \eta=0$ in its downward course; since Eqs. (2.3) and (2.5) show that $\alpha=1, \beta=0$ there, this point corresponds physically to a single bound electron in a hydrogenic $1s$ orbital, plus an electron at infinity with zero kinetic energy.

The energy $\epsilon(\eta, \lambda)$, evaluated along the four branches in Fig. 1, has been plotted in Fig. 2. Figure 3 provides an expanded view of the region around $\lambda=1$. The points B, C , and D which located vertical tangent positions for $\eta(\lambda)$ in Fig. 1 have been mapped into cusps.

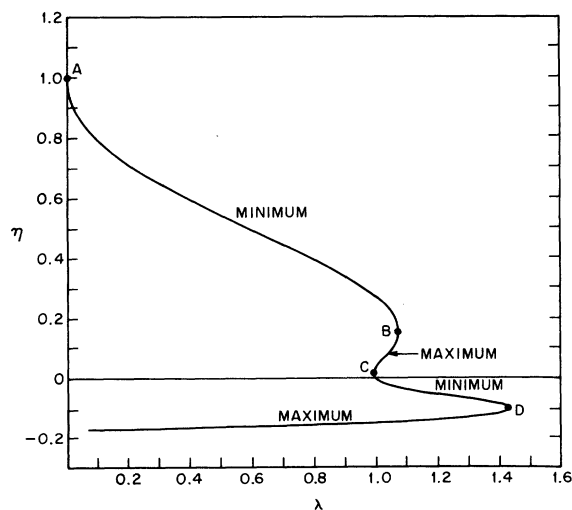


FIG. 1. Extrema for the Hylleraas-Eckart-Chandra-sekhar wave function, Eq. (2.1). The uppermost branch AB is the one which yields valid approximate wave functions and energies for the physical states $\lambda=1, \frac{1}{2}, \frac{1}{3}$, etc.

The "physical" branch AB for the energy indicates binding for the hydride ion at $\lambda=1$. Specifically, the calculations show that

$$\epsilon^{(0)}(\lambda=1) = -0.513\ 302\ 8855, \quad (2.9)$$

well below the ionization limit $-\frac{1}{2}$. Actually very accurate calculations devoted specifically to this ion¹⁷ suggest that the correct value should be

$$\epsilon^{(0)}(\lambda=1) = -0.527\ 751\ 014. \quad (2.10)$$

The error in result (2.9) for wave function (2.1) can be ascribed mostly to lack of angular correlation.¹⁵

The "physical" energy curve AB in Figs. 2 and 3 crosses the continuum edge ($\epsilon = -\frac{1}{2}$) when λ increases to

$$\lambda_c = 1.048\ 486. \quad (2.11)$$

This result should be compared to the analogous quantity proposed earlier⁶ for the exact ground-state energy, namely,

$$\lambda_c = 1.0975. \quad (2.12)$$

Although the ionization potential is predicted to go to zero at λ_c , the wave function remains bound and localized (i.e. it remains normalizable). Analytic continuation in λ , through λ_c , is possible and evidently produces bound states in the continuum. This situation persists until point B is reached.

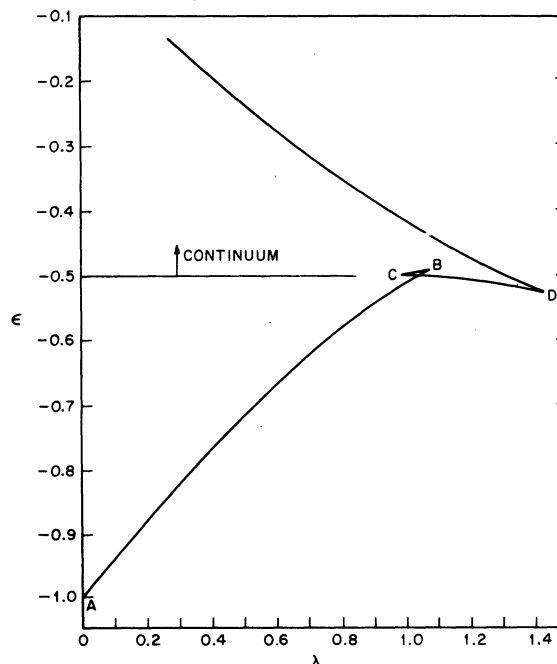


FIG. 2. Energy curves corresponding to the extremals shown in Fig. 1. Points A, B, C , and D are mappings of points with the same names in Fig. 1.

Consequently, we identify the λ value at point B , shown in Eq. (2.7), as an approximation to the exact-problem quantity λ^* of Eq. (1.4) which also represents the limit for bound states in the continuum.

Equations (2.3) and (2.5) have been used to evaluate the orbital exponents α and β along the four extremal curves. The results are displayed in Fig. 4.

In order to clarify the confluence phenomenon at point B , a family of $\epsilon(\eta, \lambda)$ curves versus η are shown in Fig. 5. These are plots of the function shown in Eq. (2.6), for five λ choices centered about the critical value $\lambda(B)$ given in Eq. (2.7), and separated by λ increments of ± 0.01 . The extrema are indicated by vertical arrows. The $\lambda(B)$ curve possesses only a horizontal point of inflection at

$$\eta(B) = 0.15414 \tag{2.13}$$

in the neighborhood of which the curve is cubic.

Since the two-variable function $\epsilon(\eta, \lambda)$ is non-singular near $\eta(B), \lambda(B)$, it may be expanded in a double Taylor series about that point:

$$\begin{aligned} \epsilon(\eta, \lambda) &= A_0 + A_1 \Delta\lambda + A_2 \Delta\lambda \Delta\eta + A_3 (\Delta\eta)^2 + \dots, \\ \Delta\lambda &= \lambda - \lambda(B), \quad \Delta\eta = \eta - \eta(B). \end{aligned} \tag{2.14}$$

The coefficients appearing in this expansion have been found to have the values

$$\begin{aligned} A_0 &= -0.4934154015, \\ A_1 &= 0.1705082019, \\ A_2 &= 1.155, \\ A_3 &= 2.384. \end{aligned} \tag{2.15}$$

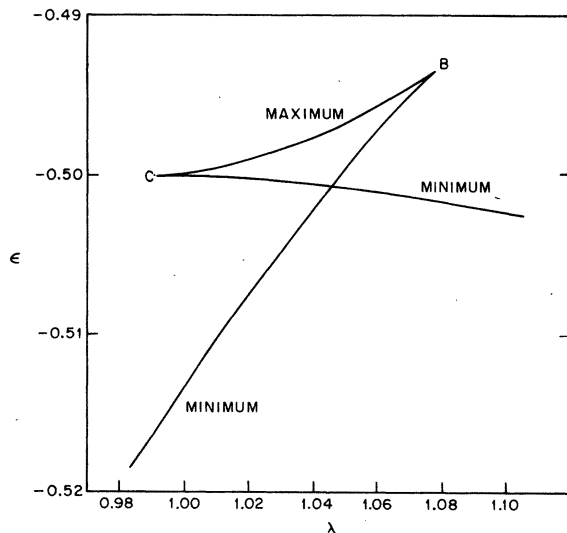


FIG. 3. Expanded view of the energy curves in the region around $\lambda = 1$.

If interest is confined to the immediate neighborhood of $\eta(B), \lambda(B)$, the explicitly shown terms in Eq. (2.14) will alone give an adequate representation for $\epsilon(\eta, \lambda)$. They imply that $\partial\epsilon/\partial\eta$ vanishes when

$$\Delta\eta = \pm(-A_2 \Delta\lambda / 3A_3)^{1/2}. \tag{2.16}$$

These extrema are real when $\lambda \leq \lambda(B)$, with the upper sign corresponding to a minimum, and the lower sign to a maximum. By substituting expression (2.16) in (2.14), the extremal energy values are found to be

$$\epsilon(\lambda) = A_0 + A_1 \Delta\lambda \mp 2A_3 (-A_2 \Delta\lambda / 3A_3)^{3/2} + O((\Delta\lambda)^2). \tag{2.17}$$

This result demonstrates that point B is a branch point of order $\frac{3}{2}$ for the energy, which may be compared with the apparent order $\frac{6}{5}$ adduced earlier for the analogous branch point in the exact solution.⁶

When λ exceeds $\lambda(B)$, the extremal η values represented by Eq. (2.16) move off the real axis. At the same time ϵ , Eq. (2.17), becomes complex, with an imaginary part depending on which side of the branch cut [extending from $\lambda(B)$ along the positive real axis toward infinity] one has elected to use. In particular, choosing to go below the cut produces a negative imaginary part:

$$\epsilon_{im} = -0.3094[\lambda - \lambda(B)]^{3/2} i + \dots, \tag{2.18}$$

where we have inserted numerical values (2.15) into Eq. (2.17). With a negative imaginary part, the quantum state decays in time, and we can use expression (2.18) to estimate lifetimes τ for the unstable complex:

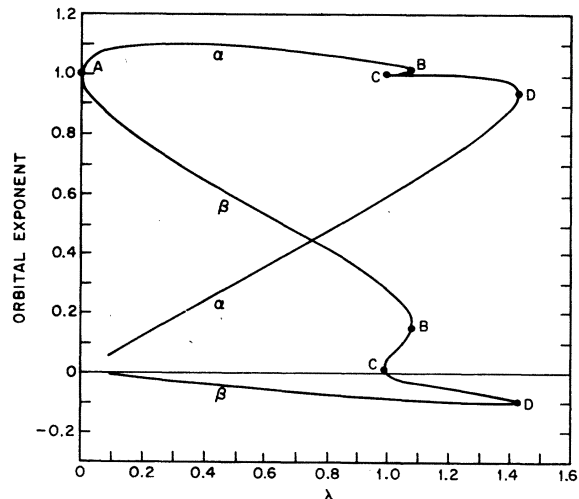


FIG. 4. Orbital exponents α and β for the Hylleraas-Eckart-Chandrasekhar wave function, Eq. (2.1).

$$\tau = \hbar / |\epsilon_{1m}|. \quad (2.19)$$

Under the assumption that the leading term shown in Eq. (2.18) affords sufficient accuracy at $\lambda = 1.5$, we calculate that the lifetime of the two-electron complex [subject to the Hamiltonian (1.1) with $n = 2$, $\lambda = 1.5 = Z^{-1}$] will be

$$\tau(\lambda = 1.5) = 6.42 \times 10^{-16} \text{ sec.} \quad (2.20)$$

The emphasis in this section has focused attention largely on the existence of a binding limit when the coupling constant reaches a sufficiently large, positive value $\lambda(B)$. However the reader should remain aware that the customary λ power series themselves can also be developed for the Hylleraas-Eckart-Chandrasekhar approximate wave function. We note in passing that the expression (2.6) for $\epsilon(\eta, \lambda)$ may be used as the basis for a small- λ iterative development, with the end result that the ground-state energy (the "physical" branch) has the expansion¹⁸:

$$\epsilon^{(0)}(\lambda) = -1 + \frac{5}{8}\lambda - \frac{31}{256}\lambda^2 - \frac{13}{2048}\lambda^3 - \frac{1513}{393216}\lambda^4 - \dots \quad (2.21)$$

If this series were extended to sufficiently high order, the set of coefficients could be used to identify the position and the nature of the singularity nearest the origin. Although it is our opinion that the branch point at $\lambda(B)$ fulfills this role (as does its analog in the exact solution), strict confirmation would require generalizing our numerical study to complex λ .

III. EXCITED STATES FOR TWO ELECTRONS

The variational principle may directly be applied to excited states, provided those states are the

lowest ones in energy for separate symmetry classes. We have numerically studied four excited states, for two electrons, which meet this criterion. In order that each of these states be described on a basis consistent with that used for the ground state, two orbital parameters were included in the respective variational wave functions. As before, the energy was minimized for each value of λ with respect to these nonlinear parameters.

In order to provide a common descriptive language for the four states, we define the mutually orthogonal atomic orbitals,

$$\begin{aligned} u(r, \alpha) &= e^{-\alpha r}, \\ v(r, \beta) &= \left[\frac{3}{\alpha + \beta} - r \right] e^{-\beta r}, \\ w_x(\vec{r}, \gamma) &= x e^{-\gamma r}, \end{aligned} \quad (3.1)$$

with w_y and w_z defined analogously. Each variational wave function ψ has been synthesized from a pair of these orbitals. Indeed the Hylleraas-Eckart-Chandrasekhar function could be considered in this light as the combination

$$u(r_1, \alpha)u(r_2, \beta) + u(r_1, \beta)u(r_2, \alpha). \quad (3.2)$$

Suppose that α_1 and α_2 are the orbital parameters occurring in ψ for a given state. We require the following matrix elements:

$$\begin{aligned} N(\alpha_1, \alpha_2) &= \langle \psi | \psi \rangle, \\ I_n(\alpha_1, \alpha_2) &= \langle \psi | r_1^{-1} + r_2^{-1} | \psi \rangle, \\ I_e(\alpha_1, \alpha_2) &= \langle \psi | r_{12}^{-1} | \psi \rangle, \\ I_k(\alpha_1, \alpha_2) &= \langle \psi | \nabla_1^2 + \nabla_2^2 | \psi \rangle. \end{aligned} \quad (3.3)$$

In each case, these matrix elements will be homo-

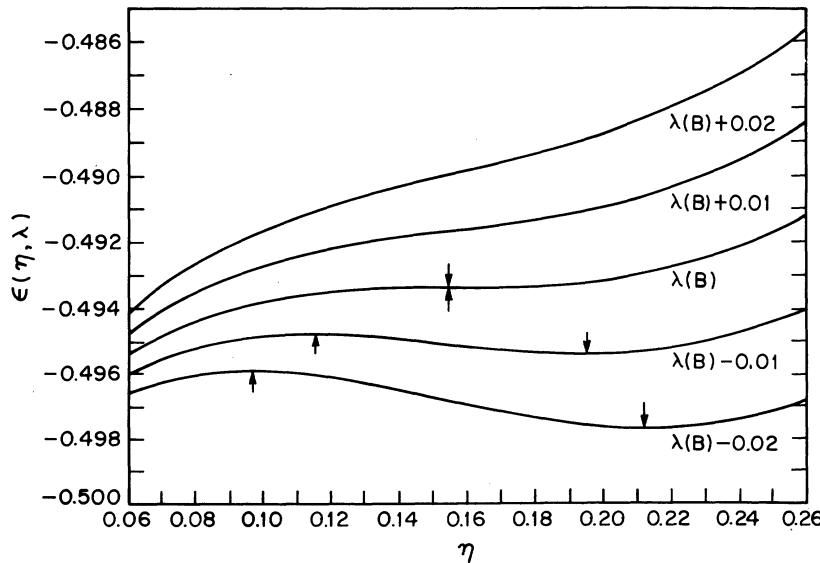


FIG. 5. Energy curves vs η , for several values of the coupling constant λ in the neighborhood of $\lambda(B) = 1.0780113$. Maxima and minima are indicated by vertical arrows pointing, respectively, upward and downward.

geneous functions of α_1 and α_2 . Setting

$$\eta = \alpha_2/\alpha_1, \quad (3.4)$$

we have

$$\begin{aligned} N(\alpha_1, \alpha_2) &= \alpha_1^{-p} N(1, \eta), \\ I_n(\alpha_1, \alpha_2) &= \alpha_1^{1-p} I_n(1, \eta), \\ I_e(\alpha_1, \alpha_2) &= \alpha_1^{1-p} I_e(1, \eta), \\ I_k(\alpha_1, \alpha_2) &= \alpha_1^{2-p} I_k(1, \eta), \end{aligned} \quad (3.5)$$

where p is an integer. The variational energy therefore becomes

$$\begin{aligned} \epsilon^{(\nu)}(\alpha_1, \alpha_2, \lambda) &= \langle \psi | H(\lambda) | \psi \rangle / \langle \psi | \psi \rangle, \\ &= [-\frac{1}{2} I_k(1, \eta) \alpha_1^2 - I_n(1, \eta) \alpha_1 \\ &\quad + \lambda I_e(1, \eta) \alpha_1] / N(1, \eta). \end{aligned} \quad (3.6)$$

This quadratic form in α_1 will be minimized when

$$\alpha_1 = [-I_n(1, \eta) + \lambda I_e(1, \eta)] / I_k(1, \eta), \quad (3.7)$$

and this value automatically causes the virial theorem to be satisfied.¹⁶

By substituting Eq. (3.7) for α_1 into Eq. (3.6), one obtains

$$\epsilon^{(\nu)}(\eta, \lambda) = \frac{[-I_n(1, \eta) + \lambda I_e(1, \eta)]^2}{2N(1, \eta) I_k(1, \eta)}. \quad (3.8)$$

An expression of this type was extremalized with respect to η for each of the four excited states, which we now discuss sequentially.

A. (1s)(2s) ³S

Triplet states require the spatial wave function to be antisymmetric with respect to electron interchange. Consequently, we take

$$\psi[(1s)(2s) {}^3S] = u(r_1, \alpha) v(r_2, \beta) - v(r_1, \beta) u(r_2, \alpha), \quad (3.9)$$

and identify $\alpha = \alpha_1$, $\beta = \alpha_2$, $\eta = \beta/\alpha$. One finds

$$\begin{aligned} N(\alpha, \beta) &= \frac{6\pi^2(\alpha^2 - \alpha\beta + \beta^2)}{\alpha^3\beta^5(\alpha + \beta)^2}, \\ I_n(\alpha, \beta) &= \frac{3\pi^2(2\alpha^3 - \alpha^2\beta + 3\beta^3)}{\alpha^3\beta^5(\alpha + \beta)^2}, \\ I_e(\alpha, \beta) &= \frac{3\pi^2(\alpha^4 + \alpha^3\beta + 4\alpha\beta^3 + 2\beta^4)}{\alpha^2\beta^4(\alpha + \beta)^5} - \frac{24\pi^2}{(\alpha + \beta)^7}, \\ I_k(\alpha, \beta) &= \frac{2\pi^2(-3\alpha^4 + 3\alpha^3\beta - 4\alpha^2\beta^2 + \alpha\beta^3 - 7\beta^4)}{\alpha^3\beta^5(\alpha + \beta)^2}. \end{aligned} \quad (3.10)$$

The exact unperturbed wave function is obtained for $\alpha = 1$, $\beta = \frac{1}{2}$, and the corresponding energy is $\epsilon = -\frac{5}{8}$. Figure 6 shows that the computed η declines monotonically as λ increases from zero,

and exhibits a simple zero at $\lambda = 1$. We have discovered no analog of the vertical tangent behavior shown earlier for the ground-state η ; indeed η for this excited state continues its downward drift until λ is at least 10.

The energy versus λ is shown in Fig. 7, and the orbital parameters appear in Fig. 8.

This excited state presents a behavior that is obviously distinct from the pattern established by the ground state. Most importantly, the hydride ion is not bound in this state, as has been known for some time.¹⁷ This is manifest in the present calculations by tangency of the energy curve, Fig. 7, to the continuum edge at $-\frac{1}{2}$, precisely when $\lambda = 1$. That the state should lie below this continuum edge for any $\lambda < 1$ follows from the fact that the nucleus plus core electron present a net positive charge [$1 - \lambda$ in units for which $H(\lambda)$ is written in Eq. (1.1)] which can always bind the outer electron in any one of an infinite number of extended hydrogenic orbitals. The decrease of orbital exponent β through zero at $\lambda = 1$ confirms that fact.

Evidently, analytic continuation through $\lambda = 1$ is possible for wave function and energy. The present example therefore seems to conform to the general critical binding phenomenon that has been analyzed by Lekner.¹⁹ By virtue of the negative β values obtained by the continuation, the wave function has ceased to be normalizable.

Although no singularity was encountered along the positive real λ axis, singularities may well occur in the complex λ plane relatively close to the origin. In this connection the near-hyperbolic shape of the energy curve given in Fig. 7 is suggestive. Near $\lambda = 1$, this energy is very roughly equal to the hyperbolic function,

$$-0.47 - 0.15[(\lambda - 1)^2 + (0.2)^2]^{1/2}, \quad (3.11)$$

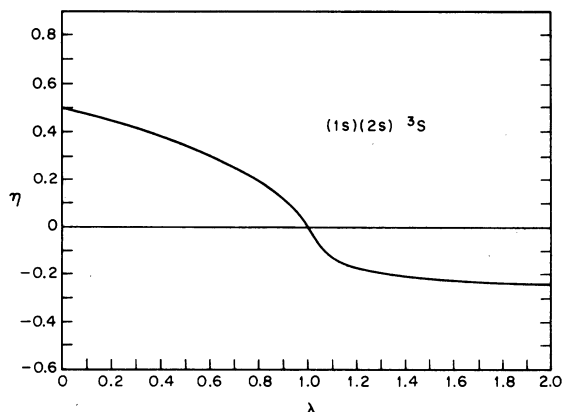


FIG. 6. Extremal values of the nonlinear variational parameter η for the (1s) (2s) ³S excited state for two electrons.

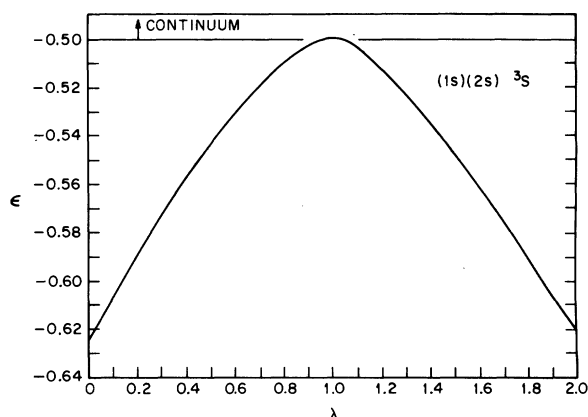


FIG. 7. Energy for the two-electron excited state $(1s)(2s)^3S$, determined variationally from the wave function (3.9).

which possesses a complex conjugate pair of branch points at

$$\lambda = 1 \pm 0.2i. \quad (3.12)$$

It should be noted in passing that such a pair of singularities near the real axis, if they are the closest singularities to the origin, will produce perturbation coefficients with signs that alternate slowly with increasing order; interestingly, that seems to be the behavior obtained recently by Middal, Lyslo, and Aashamar in their exhaustive study of the perturbation coefficients.²⁰

B. $(1s)(2p)^3P$

The antisymmetric wave function was taken to be

$$\psi[(1s)(2p)^3P] = u(r_1, \alpha)w_x(\vec{r}_2, \beta) - w_x(\vec{r}_1, \beta)u(r_2, \alpha). \quad (3.13)$$

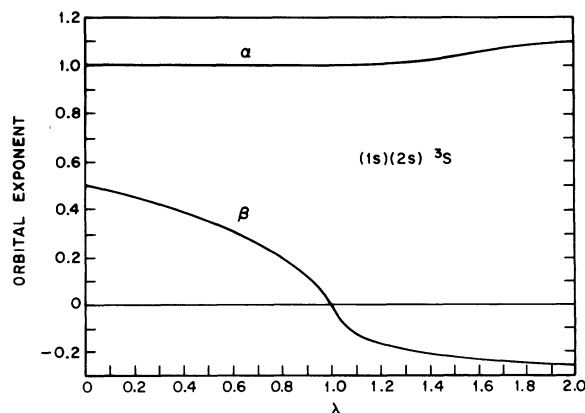


FIG. 8. Orbital exponents for the variational wave function (3.9) representing the two-electron excited state $(1s)(2s)^3S$.

The required integrals generated by this choice are the following:

$$\begin{aligned} N(\alpha, \beta) &= \frac{2\pi^2}{\alpha^3\beta^5}, \\ I_n(\alpha, \beta) &= \frac{\pi^2(2\alpha + \beta)}{\alpha^3\beta^5}, \\ I_e(\alpha, \beta) &= \frac{\pi^2}{(\alpha + \beta)^5} \left(\frac{\alpha^4 + 5\alpha^3\beta + 10\alpha^2\beta^2 + 10\alpha\beta^3 + 2\beta^4}{\alpha^2\beta^4} \right. \\ &\quad \left. - \frac{56}{3(\alpha + \beta)^2} \right), \\ I_h(\alpha, \beta) &= -\frac{2\pi^2(\alpha^2 + \beta^2)}{\alpha^3\beta^5}. \end{aligned} \quad (3.14)$$

The unperturbed values for α and β are 1 and $\frac{1}{2}$, respectively, giving $\epsilon(\lambda=0) = -\frac{5}{8}$. Our calculations show that $\eta = \beta/\alpha$ declines monotonically for real positive λ without interruption, in a manner closely analogous to that encountered above for $(1s)(2s)^3S$. Figure 9 shows that behavior, while Fig. 10 gives the energy, and Fig. 11 the separate orbital exponents α and β . This is clearly another case for which the hydride ion ($\lambda=1$) has vanishing ionization potential, with energy that is locally quadratic at this point of tangency to the continuum edge. As before, analytic continuation through $\lambda=1$ is possible to a regime with a nonintegrable wave function.

C. $(1s)(2p)^1P$

This case differs from the preceding one only by change of sign in ψ :

$$\psi[(1s)(2p)^1P] = u(r_1, \alpha)w_x(\vec{r}_2, \beta) + w_x(\vec{r}_1, \beta)u(r_2, \alpha), \quad (3.15)$$

to produce a spatial function symmetric under electron interchange. The integrals N , I_n , and I_h are unchanged by this modification, so the expres-

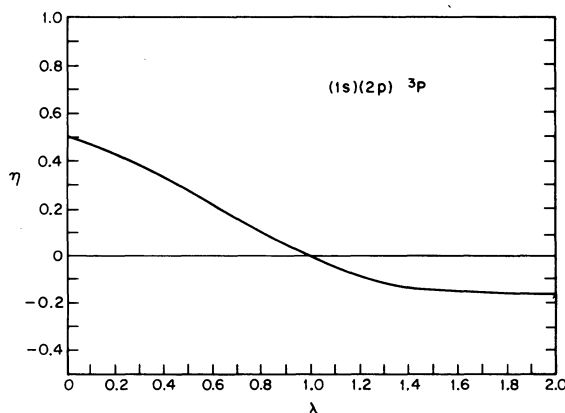


FIG. 9. Extremal values of variational parameter $\eta = \beta/\alpha$, for the two-electron excited state $(1s)(2p)^3P$.

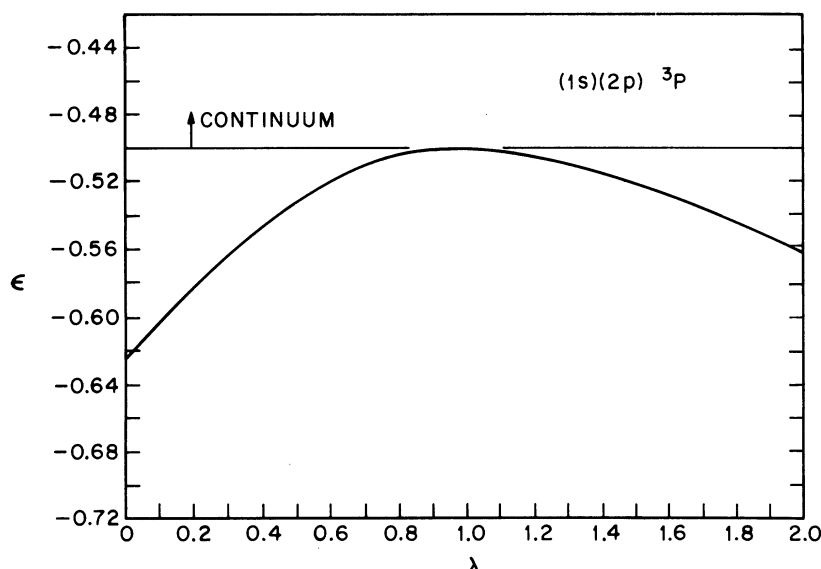


FIG. 10. Energy for the two-electron excited state $(1s)(2p)^3P$, corresponding to wave function (3.13).

sions (3.14) for them are still relevant. However, I_e suffers a sign change in its last term to become

$$I_e(\alpha, \beta) = \frac{\pi^2}{(\alpha + \beta)^5} \left(\frac{\alpha^4 + 5\alpha^3\beta + 10\alpha^2\beta^2 + 10\alpha\beta^3 + 2\beta^4}{\alpha^2\beta^4} + \frac{56}{3(\alpha + \beta)^2} \right). \quad (3.16)$$

This state shares, with the preceding two excited states $(1s)(2s)^3S$ and $(1s)(2p)^3P$, vanishing of the ionization potential as λ approaches 1. Likewise η and β have simple zeros there, and analytic continuation through $\lambda = 1$ leads to $\beta < 0$ and a non-normalizable wave function. Figures 12, 13, and 14 show the detailed behavior of η , α and β , and ϵ , respectively.

A surprising new feature is the appearance of a

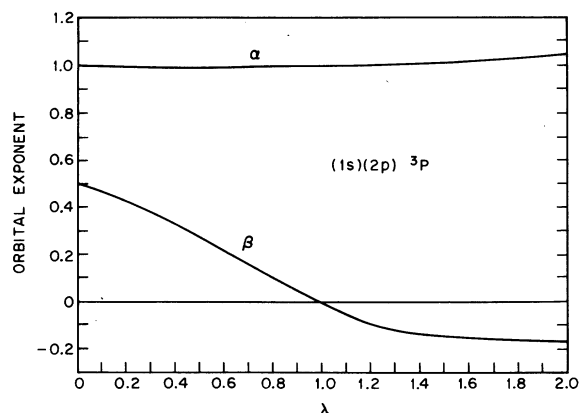


FIG. 11. Orbital exponents for variational wave function (3.13), representing the two-electron excited state $(1s)(2p)^3P$.

branch point on the positive real λ axis, at

$$\lambda = 1.182144, \quad (3.17)$$

within the non-normalizable regime. This point is analogous to point *B* discussed previously for the ground state, in that the η , α and β curves develop vertical tangents there as a result of confluence with maximum branches. Also following the ground-state pattern, the energy possesses a $\frac{3}{2}$ -power cusp at this point.

If the approximate power-series coefficients (available from extensive variation-perturbation calculations²⁰) are any indication, the positive-real-axis singularity (3.17) is not the nearest one to $\lambda = 0$. Instead, at least one pair of complex con-

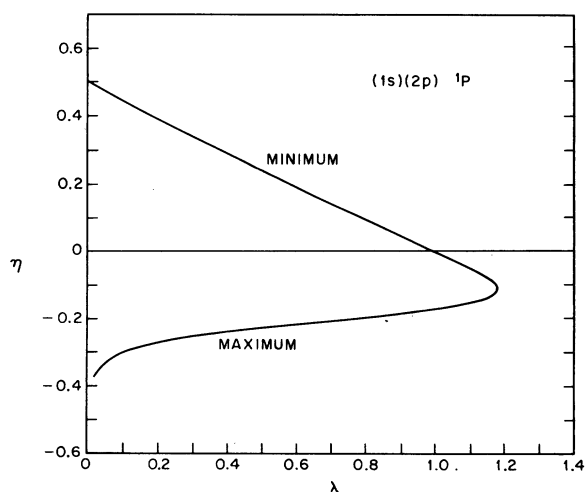


FIG. 12. Extremal values of $\eta = \beta/\alpha$ for the two-electron excited state $(1s)(2p)^1P$.

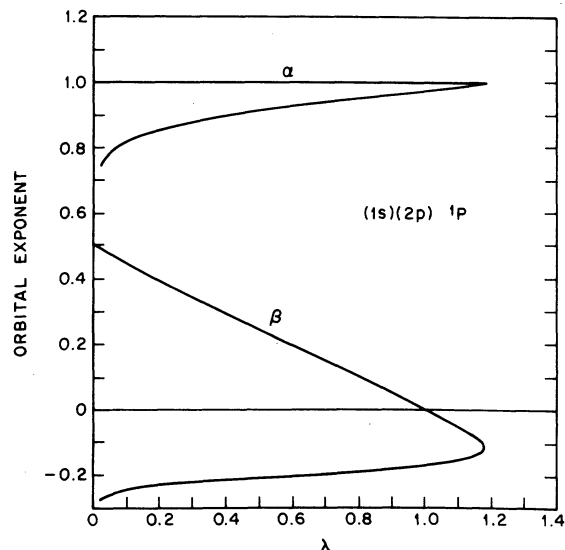


FIG. 13. Orbital exponents α and β for the two-electron excited state $(1s)(2p)^1P$. For each, the upper branch corresponds to the "physical" energy minimum, and the lower branch to an unphysical energy maximum.

jugate singularities seems to fill that role. If this is indeed the case, our nonlinear variation calculation (though approximate) effects analytic continuation beyond the convergence radius for the perturbation power series.

D. $(2p)^2\ ^3P$

This is the only excited state known definitely to be bound for the hydride anion, though its ion-

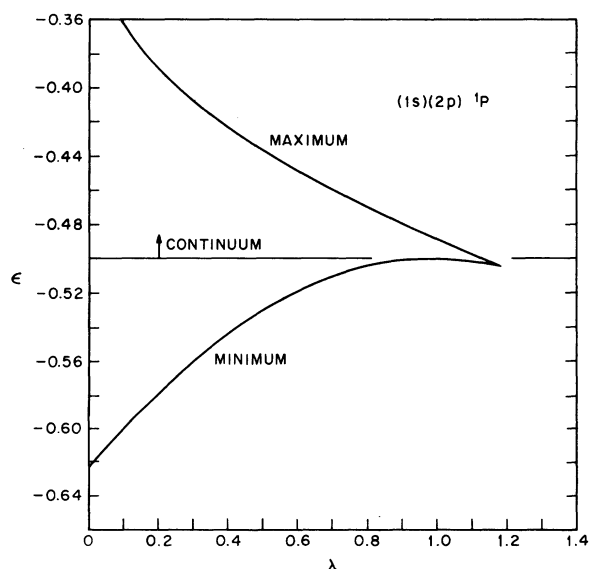


FIG. 14. Energy for the two-electron excited state $(1s)(2p)^1P$.

ization potential is only about one-eightieth that of the ground state.² In the present series of calculations, it was assumed that the antisymmetric wave function could be approximated adequately by:

$$\begin{aligned} \psi[(2p)^2\ ^3P] = & w_x(\vec{r}_1, \alpha)w_x(\vec{r}_2, \beta) - w_x(\vec{r}_1, \alpha)w_x(\vec{r}_2, \beta) \\ & + w_x(\vec{r}_1, \beta)w_x(\vec{r}_2, \alpha) - w_x(\vec{r}_1, \beta)w_x(\vec{r}_2, \alpha). \end{aligned} \quad (3.18)$$

This in turn leads to the following integrals:

$$\begin{aligned} N(\alpha, \beta) &= 4\pi^2 \left(\frac{1}{\alpha^5\beta^5} + \frac{1024}{(\alpha+\beta)^{10}} \right), \\ I_n(\alpha, \beta) &= 2\pi^2 \left(\frac{\alpha+\beta}{\alpha^5\beta^5} + \frac{1024}{(\alpha+\beta)^9} \right), \\ I_e(\alpha, \beta) &= \frac{2\pi^2(\alpha^4 + 5\alpha^3\beta + 9\alpha^2\beta^2 + 5\alpha\beta^3 + \beta^4)}{\alpha^4\beta^4(\alpha+\beta)^5} \\ &\quad + \frac{672\pi^2}{(\alpha+\beta)^9}, \\ I_k(\alpha, \beta) &= -4\pi^2 \left(\frac{\alpha^2 + \beta^2}{\alpha^5\beta^5} + \frac{2048\alpha\beta}{(\alpha+\beta)^{10}} \right). \end{aligned} \quad (3.19)$$

Figures 15-17 show the computed results. It is striking how similar they are to their ground-state analogs. In particular, singular points A' , B' , C' , and D' can be identified, which are the analogs of A , B , C , and D in the earlier Figs. 1-4. The following values were found for the coupling strength at these singular points:

$$\lambda(B') = 0.9842, \quad \lambda(C') = 0.9502, \quad \lambda(D') = 1.3994. \quad (3.20)$$

Considering how small the exact ionization poten-

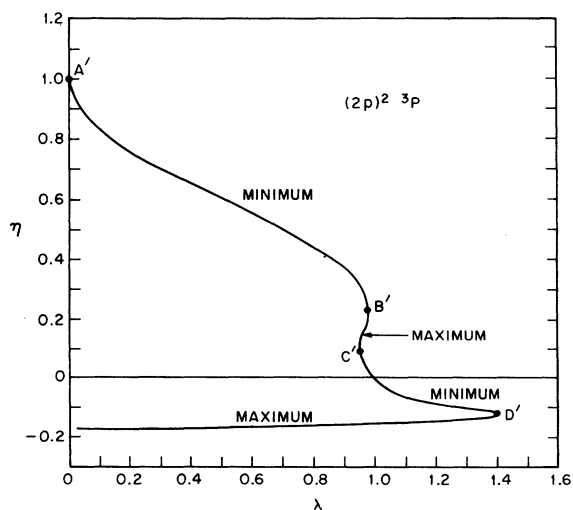


FIG. 15. Extremal values of $\eta = \beta/\alpha$ for the two-electron excited state $(2p)^2\ ^3P$.

tial at $\lambda=1$ is for this excited state, a very flexible (and consequently very accurate) variational wave function would be required to produce any binding at $\lambda=1$. The trial function (3.18) does not possess sufficient flexibility for that purpose. Nevertheless it is significant that function (3.18) has produced the same sort of singularity in the continuum, for real positive λ , that occurs for the ground state. We believe that a sequence of improved variational calculations for $(2p)^2\ ^3P$ will cause $\lambda(B')$ to increase beyond unity, so as to come into close agreement with the singular point

$$\lambda^* = 1.0128 \quad (3.21)$$

that has been inferred⁶ from the accurate λ power-series coefficients.²

IV. THREE-ELECTRON GROUND STATE

The preceding calculations seem to suggest a general code of behavior: If the anion is bound, the state remains normalizable as λ increases and enters the continuum, terminating finally at a branch point. On the other hand if the anion [$\lambda=1$ for two electrons, $\lambda=1/(n-1)$ for n electrons] is unbound the energy curve is tangent to the continuum and the point of tangency marks the onset of wave-function non-normalizability.

We have examined the three-electron ground state, to see if its results were consistent with the proposed behavior.

Including both spin and space coordinates, the doublet eigenfunctions for three electrons conform to the following structure:

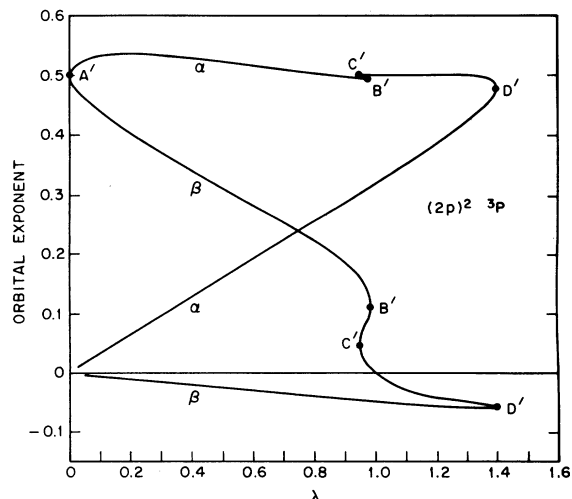


FIG. 16. Orbital exponents for the two-electron excited state $(2p)^2\ ^3P$.

$$\begin{aligned} \psi(123) = & f(\vec{r}_1, \vec{r}_2 | \vec{r}_3) \alpha(1) \alpha(2) \beta(3) \\ & + f(\vec{r}_3, \vec{r}_1 | \vec{r}_2) \alpha(1) \beta(2) \alpha(3) \\ & + f(\vec{r}_2, \vec{r}_3 | \vec{r}_1) \beta(1) \alpha(2) \alpha(3). \end{aligned} \quad (4.1)$$

The spatial function f is required to satisfy two conditions²¹:

$$f(\vec{r}_2, \vec{r}_1 | \vec{r}_3) = -f(\vec{r}_1, \vec{r}_2 | \vec{r}_3); \quad (4.2)$$

$$f(\vec{r}_1, \vec{r}_2 | \vec{r}_3) + f(\vec{r}_3, \vec{r}_1 | \vec{r}_2) + f(\vec{r}_2, \vec{r}_3 | \vec{r}_1) = 0. \quad (4.3)$$

The first ensures over-all antisymmetry for ψ , while the second automatically removes quartet spin character from ψ .

The ground state for three electrons has the designation $(1s)^2(2s)^2S$. It may be variationally approximated by selecting f to be a suitable combination of the orbitals defined in Eq. (3.1). The specific form used was

$$\begin{aligned} f(\vec{r}_1, \vec{r}_2 | \vec{r}_3) = & [u(r_1, \alpha) v(r_2, \beta) \\ & - v(r_1, \beta) u(r_2, \alpha)] u(r_3, \alpha), \end{aligned} \quad (4.4)$$

which identically satisfies conditions (4.2) and (4.3).

The earlier formulas (3.7) and (3.8) are once again relevant, with $\alpha_1 = \alpha$ and $\eta = \beta/\alpha$. For the present case, the various integrals are found to be²²:

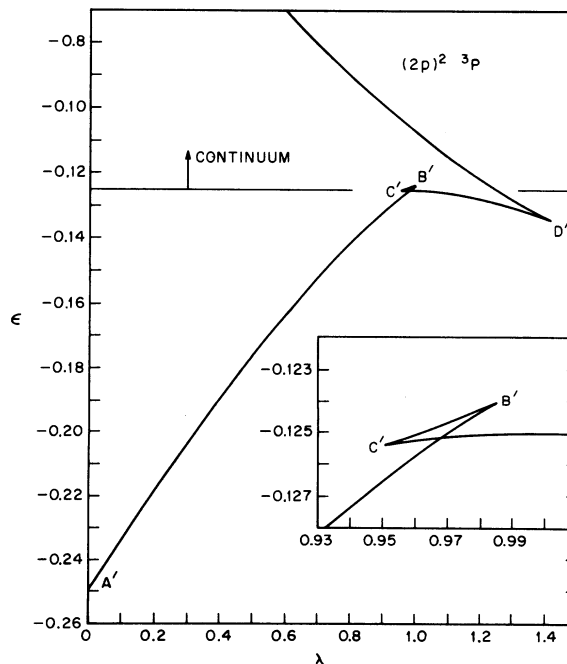


FIG. 17. Energy for the two-electron excited state $(2p)^2\ ^3P$. The inset provides an expanded view of the region near $\lambda=0.97$.

$$\begin{aligned}
 N(\alpha, \beta) &= \langle f | f \rangle \\
 &= \frac{6\pi^3(\alpha^2 - \alpha\beta + \beta^2)}{\alpha^6\beta^5(\alpha + \beta)^2}, \\
 I_n(\alpha, \beta) &= \langle f | \frac{1}{r_1} + \frac{1}{r_2} + \frac{1}{r_3} | f \rangle, \\
 &= \frac{3\pi^3(4\alpha^3 - 3\alpha^2\beta + 2\alpha\beta^2 + 3\beta^3)}{\alpha^6\beta^5(\alpha + \beta)^2}, \\
 I_e(\alpha, \beta) &= \langle f | \frac{1}{r_{12}} + \frac{1}{r_{13}} + \frac{1}{r_{23}} | f \rangle, \quad (4.5) \\
 &= \frac{6\pi^3(\alpha^4 + \alpha^3\beta + 4\alpha\beta^3 + 2\beta^4)}{\alpha^5\beta^4(\alpha + \beta)^5} \\
 &\quad + \frac{15\pi^3(\alpha^2 - \alpha\beta + \beta^2)}{4\alpha^5\beta^5(\alpha + \beta)^2} - \frac{24\pi^3}{\alpha^3(\alpha + \beta)^7}, \\
 I_k(\alpha, \beta) &= \langle f | \nabla_1^2 + \nabla_2^2 + \nabla_3^2 | f \rangle \\
 &= -\frac{2\pi^3(6\alpha^4 - 6\alpha^3\beta + 7\alpha^2\beta^2 - \alpha\beta^3 + 7\beta^4)}{\alpha^6\beta^5(\alpha + \beta)^2}.
 \end{aligned}$$

The continuum edge for the preceding two-electron states was always a λ -independent constant; now it is the ground-state energy of the two-electron system remaining after ionization of the third electron. In the present approximation, that continuum edge is represented by

$$\epsilon_c(\lambda) = -(1 - \frac{5}{16}\lambda)^2. \quad (4.6)$$

For the λ range of primary interest (near $\frac{1}{2}$), this should be an adequately precise description.

Figures 18, 19, and 20 show the results, respectively, for η , α and β , and ϵ . They imply that the He^- anion is not bound, and this agrees with experiment, apparently.²³ The orbital exponent β becomes negative beyond $\lambda = \frac{1}{2}$, while the energy is tangent to the continuum at this point. Therefore the three-electron ground state seems to con-

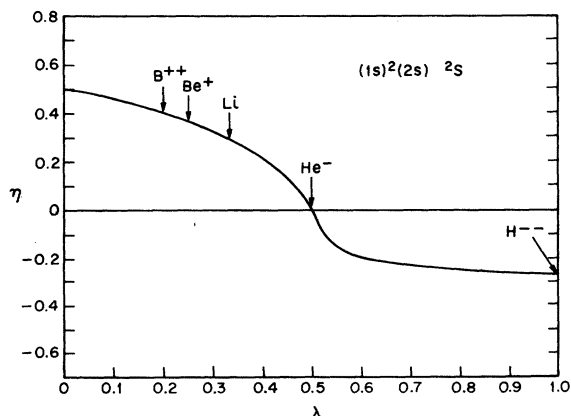


FIG. 18. Extremal values of $\eta = \beta/\alpha$ for the ground state of the three-electron system.

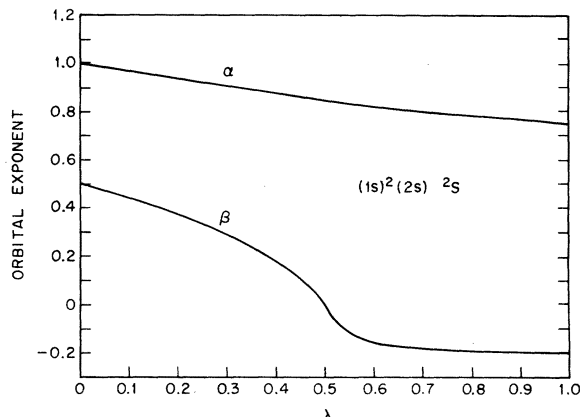


FIG. 19. Orbital exponents for the ground state of the three-electron system.

form to the second half of the theme established by our two-electron calculations.

As a measure of the accuracy of the orbital approximation (4.4) to describe the three-electron ground state, we can compare the predicted and measured ionization potentials for lithium ($\lambda = \frac{1}{3}$). Our calculation implies 5.20245 eV, which compares moderately well with the experimental value 5.388 eV.²⁴

A metastable bound state for He^- has been reported,²³ and assigned to the state $(1s)(2s)(2p)^4P$. This state should be the lowest in energy for its symmetry, and therefore would be amenable to direct variational study along the lines pursued in this paper. We anticipate that a branch point will be found on the positive λ axis, with an energy that has risen into the relevant continuum, to exemplify the first half of our general theme.

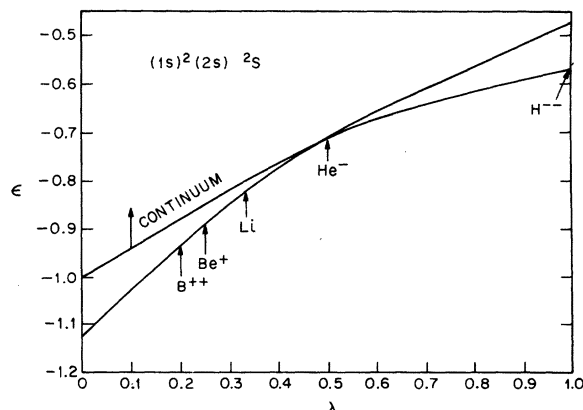


FIG. 20. Ground-state energy of the three-electron system. The continuum edge is defined by the parabola $-(1 - 5\lambda/16)^2$, in the present approximation.

V. DISCUSSION

The purpose of the present paper has been to demonstrate the relevance of simple nonlinear variational calculations to the study of quantum-mechanical perturbation theory with arbitrary coupling strength. Although we believe the results are qualitatively significant, it will be necessary to use more elaborate trial wave functions to achieve more impressive numerical accuracy. It should be obvious that each elaboration complicates the numerical analysis by introducing further variational parameters that with their predecessors require simultaneous extremalizing.

For those eigenstates which possess branch points on the positive λ axis, we expect normally to find that any wave function of finite complexity will produce energy branch points with characteristic exponent $\frac{3}{2}$. However, it appears that the exact $\epsilon^{(\nu)}(\lambda)$ can exhibit somewhat different powers.⁶ These modified exponents then must arise as a property of that limit in which arbitrary flexibility is present in the trial wave function, and for which the energy must be extremalized over a parameter space of infinite dimensionality.

Each calculation presented in this paper involved only two variational parameters at the outset. Considerations related to the virial theorem reduced the dimensionality to one. Energy extrema in the one-dimensional (η) space could only be simple minima or maxima (except at the precise point of confluence when a horizontal point of inflection obtains). But with a number $q > 2$ of variational parameters in ψ , energy extrema in the reduced space with dimensionality $q - 1 > 1$ can be of several types, depending on the signs of principal curvatures. The resulting normal circumstance whereby a singular point would develop for a "physical" energy branch, would entail confluence of a relative minimum (all curvatures positive) with a saddle point (one curvature negative, the others positive). These considerations suggest that considerable care should henceforth be exercised to understand the differential geometry of energy hypersurfaces in multidimensional parameter spaces.

It has not escaped our attention that the energy curves shown in Fig. 5 resemble pressure isotherms in the critical region of a condensing gas described, for example, by the van der Waals equation of state.²⁵ Indeed the mathematical singularity of the energy, for sufficiently large positive λ , is analogous to the free-energy singularity at the critical point of a many-body system which can undergo a phase change. It seems likely, therefore, that a suitable version of the renormalization-group techniques that apply to calculation

of critical exponents²⁶ could be used to clarify the singularities of the $\epsilon^{(\nu)}(\lambda)$.

The analytical perturbation theory advocated here should be useful for understanding at least some resonances in electron scattering experiments.²⁷ Heretofore, the available theoretical methods for calculating the positions and widths of scattering resonances have seemed mathematically ambiguous. However, analytic continuation of an eigenvalue $\epsilon^{(\nu)}(\lambda)$ into the continuum is unambiguous, and we have seen that the imaginary part of the energy beyond a branch point may be extracted to give the lifetime of that compound state directly.

In this regard, the ground state of the ten-electron system (corresponding to the real particles F^- , Ne, Na^+ , Mg^{++} , Al^{3+} , ...) offers a particularly interesting example. Since the singly charged anion F^- ($\lambda = \frac{1}{9}$) is bound, we expect that further increase of λ would cause penetration of the continuum and eventual encounter with a branch point. It will be valuable to determine whether this branch point λ^* occurs before λ reaches $\frac{1}{8}$, corresponding to the oxide anion O^{--} . If $\lambda^* < \frac{1}{8}$, this anion would have a finite lifetime determined by the computed imaginary part of the energy at $\lambda = \frac{1}{8}$. On the other hand, if $\lambda^* \geq \frac{1}{8}$, O^{--} would have an infinite lifetime (in the present Schrödinger-equation description). Note that although O^{--} has reportedly been observed,²⁸ its lifetime is not experimentally known.

These O^{--} results would be directly applicable to the scattering of electrons from O^- . The real part of the ten-electron energy analytically continued to $\lambda = \frac{1}{8}$ predicts a resonance position, equivalent to the negative electron affinity of O^- . If $\lambda^* < \frac{1}{8}$, the resonance width would be predicted by the lifetime already mentioned; if $\lambda^* \geq \frac{1}{8}$ the resonance would be extremely narrow.

It should also be mentioned that the energetics of O^{--} is important in the Born-Haber cycle for oxide crystals,²⁹ from which the negative electron affinity of O^- can be extracted. This solid-state application adds extra motivation to applying our analytical perturbation theory specifically to the ten-electron case.

Extension of the present perturbation technique to polynuclear systems opens up a rich area of further application. For example, the ability of two protons to bind three electrons depends on internuclear distance R . For large R the system readily forms $H + H^-$. But as R decreases toward the united-atom limit $R = 0$, the capacity to bind the third electron must disappear since we know He^- is not stable. Evidently the transition occurs at some $R_c > 0$ which must mark the intersection of potential-energy curves for $H + H^-$ and for $H + H$. The nature of this intersection can effectively be

studied by simultaneously considering both R and λ variations. The resulting potential curves should then be useful in analyzing inelastic $H + H^-$ collisions in which an electron is lost.³⁰

Apparently the reverse situation can also occur. Neither of two widely separated Be atoms will add an extra electron. The corresponding united atom, however, is O, which easily forms O^- . Again a critical distance R_c for binding could be identified.

In a more general context, it will probably be valuable to study the role of electron-electron repulsions via analytical perturbation theory in all

classes of chemical compounds. It seems clear that directed valence and covalent bond formation is already implicit in the $\lambda=0$ limit, which is computationally simple even for rather complicated molecules. The extent to which more subtle effects (such as hydrogen bonding, ligand field effects, and barriers to internal rotation) owe their existence to nonzero λ surely deserves to be examined in depth. Upon its essential completion, analytical perturbation theory could serve to foment a didactic revolution throughout all of structural chemistry.

*Resident visitor.

¹E. A. Hylleraas, Z. Phys. **65**, 209 (1930).

²J. Midtdal, Phys. Rev. **138**, A1010 (1965).

³T. Kato, *Perturbation Theory for Linear Operators* (Springer, New York, 1966), pp. 410–413.

⁴P. Dienes, *The Taylor Series* (Dover, New York, 1957), Chap. XIV.

⁵M. E. Fisher, Repts. Prog. Phys. **30**, 615 (1967); in particular see Sec. 7.2.

⁶F. H. Stillinger, J. Chem. Phys. **45**, 3623 (1966).

⁷E. Brändas and O. Goscinski, Int. J. Quantum Chem. **4**, 571 (1970).

⁸H. A. Bethe and E. E. Salpeter, *Quantum Mechanics of One- and Two-Electron Atoms* (Springer-Verlag, Berlin, 1957), p. 156.

⁹F. C. Sanders and C. W. Scherr, Phys. Rev. **181**, 84 (1969).

¹⁰In the case of the three-electron ground state, only ϵ_0 to ϵ_3 have been determined; see S. Seung and E. B. Wilson, Jr., J. Chem. Phys. **47**, 5343 (1967).

¹¹Reference 3, p. 120, Theorem 6.1.

¹²E. A. Hylleraas, Z. Phys. **54**, 347 (1929).

¹³C. Eckart, Phys. Rev. **36**, 878 (1930).

¹⁴S. Chandrasekhar, Astrophys. J. **100**, 176 (1944).

¹⁵F. H. Stillinger and T. A. Weber, following paper, Phys. Rev. A **10**, 1122 (1974).

¹⁶P.-O. Löwdin, Adv. Chem. Phys. **2**, 207 (1959); see

pp. 219–223.

¹⁷C. L. Pekeris, Phys. Rev. **126**, 1470 (1962).

¹⁸The exact solution for comparison (see Ref. 2) has the form $\epsilon^{(0)}(\lambda) = -1 + \frac{5}{8}\lambda - 0.157666\lambda^2 + 0.008699\lambda^3 - 0.000889\lambda^4 - \dots$

¹⁹J. Lekner, Mol. Phys. **23**, 619 (1972).

²⁰J. Midtdal, G. Lyslo, and K. Aashamar (unpublished).

²¹R. J. White and F. H. Stillinger, Phys. Rev. A **3**, 1521 (1971).

²²Since $H(\lambda)$ is spin independent, these matrix elements need only be (and were) calculated using just one of the three spin components shown in Eq. (4.1). The other components just repeat the quoted integrals.

²³R. S. Berry, Chem. Rev. **69**, 533 (1969).

²⁴L. Pauling, *The Nature of the Chemical Bond* (Cornell U.P., Ithaca, 1960), p.40.

²⁵J. O. Hirschfelder, C. F. Curtiss, and R. B. Byrd, *Molecular Theory of Gases and Liquids* (Wiley, New York, 1954), p. 364.

²⁶K. G. Wilson, Phys. Rev. B **4**, 3174, 3184 (1971).

²⁷G. J. Schulz, Rev. Mod. Phys. **45**, 378, 423 (1973).

²⁸H. Baumann, E. Heinicke, H. J. Kaiser, and K. Bethge, Nucl. Instrum. Methods **95**, 389 (1971).

²⁹Reference 24, p. 510.

³⁰We are grateful to Dr. John C. Tully for an edifying discussion of this phenomenon.